DISCRETE AND CONTINUOUS
DYNAMICAL SYSTEMS
Volume 11, Number 1, July 2004

Website: http://aimSciences.org

pp. 27–45

SINGULARITY FORMATION IN THE GENERALIZED BENJAMIN-ONO EQUATION

J.L. BONA

Department of Mathematics, Statistics and Computer Science
University of Illinois
60607-7045 Chicago, Illinois

H. KALISCH

Centre for Mathematical Sciences
Lund University
221 00 Lund, Sweden

ABSTRACT. A Fourier-collocation scheme is used to approximate solutions to the generalized Benjamin-Ono equation $u_t + u^p u_x - Hu_{xx} = 0$. The numerical simulation suggests that the equation features smooth solutions that become unbounded in finite time.

1. **Introduction.** The Benjamin-Ono equation

$$u_t + uu_x - Hu_{xx} = 0 \tag{1}$$

was derived by Benjamin [2], and later by Ono [12] as a model equation for wave motion at the interface of a two-layer fluid system, in which a finite layer of fluid is situated above or underneath an infinitely-deep layer of fluid, and the densities of the two homogeneous layers are such that the system is statically stable. The function $u(x,t)$ denotes the deviation of the interface from its rest position at the point x in the direction of propagation at time t. It is assumed that the waves do not vary significantly in the direction orthogonal to x. The variables are non-dimensional and have been normalized to reach the tidy form (1). The operator H is the Hilbert transform, given by the principal value of the integral

$$\frac{1}{\pi}\int_{-\infty}^{\infty} \frac{f(x-y)}{y}\,dy$$

for functions in $L^p(\mathbb{R})$, or by

$$\frac{1}{2\pi}\int_{-\pi}^{\pi} \cot(\tfrac{y}{2}) f(x-y)\,dy$$

in case f is periodic with period 2π say. The reader is referred to [9] for additional information about modeling aspects of (1), and a study of alternative model equations in the same situation.

In this article, the focus will be on the initial-value problem for the natural generalization

$$u_t + u^p u_x - Hu_{xx} = 0 \tag{2}$$

1991 *Mathematics Subject Classification.* 35B60.

Key words and phrases. Nonlinear Waves, Integro-Differential Equations, Fourier-Collocation, Singularity Formation.

of (1), where p is a positive integer. The competition between nonlinear and dispersive effects evident in (2) gives rise to a number of interesting phenomena, such as the existence of solitary-wave solutions. Among the more mathematical topics of investigation, the well-posedness of (2) in Sobolev function classes has been of considerable recent interest.

The Cauchy problem associated to the generalized Benjamin-Ono equation with initial value

$$u(x,0) = u_0(x), \qquad \text{for } x \in \mathbb{R} \tag{3}$$

is locally well posed in Hadamard's sense in function classes of sufficient decay and regularity. The same is true for the initial-value problem with periodic boundary conditions. For $p = 1$ it is well understood that the initial-value problem is well posed globally in time. It is also the case that the initial-value problem for (2) is globally well posed for large p and small initial data. Interest here is centered on whether or not arbitrary smooth initial data lead to a globally defined solution. By analogy with what we know about the generalized Korteweg-de Vries equation

$$u_t + u^p u_x + u_{xxx} = 0, \tag{4}$$

we expect that if $p \geq 2$ in (2) and the initial data u_0 in (3) are large enough, then the solution need not be globally defined, no matter how smooth it may be initially. This issue is investigated by numerical simulation, much in the vein of the study of (4) in [3]. The plan of the paper is as follows. In Section 2, some facts regarding the initial-value problem are reviewed. Section 3 is devoted to the description of the numerical scheme and Section 4 contains some convergence and accuracy tests. The heart of the paper is Section 5, where a strong case is made for the appearance of singularity formation.

2. **Overview of well-posedness results.** The initial-value problem

$$\left.\begin{aligned} u_t + u^p u_x - Hu_{xx} = 0, \\ u(x,0) = u_0(x), \end{aligned}\right\} \tag{5}$$

for $x \in \mathbb{R}$ and $t \in [0,T]$, is known to be locally well-posed in the standard Sobolev spaces $H^s(\mathbb{R})$ and $H^s_\#([0,2\pi])$ when $s > \frac{3}{2}$. The space $H^s_\#([0,2\pi])$ is comprised of the elements of $H^s_{loc}(\mathbb{R})$ which are 2π-periodic, and is equipped with the obvious norm. In the case $p = 1$, the problem is well-posed globally in time. The proof of this fact makes use of the well-known infinite family of conserved integrals as explained in [1], for instance. The first four of these are

$$\begin{aligned} I_{-1}(u) &= \int u, \\ I_0(u) &= \int u^2, \\ I_1(u) &= \tfrac{1}{3}\int u^3 - \int uHu_x, \\ I_2(u) &= \tfrac{1}{4}\int u^4 - \tfrac{3}{2}\int u^2 Hu_x + 2\int u_x^2. \end{aligned}$$

The unadorned integral stands for integration with respect to the spatial variable x over $\mathbb{R}$ or $[0,2\pi]$, depending on whether solutions on the line or with periodic initial conditions are considered. These conserved integrals are used to obtain *a priori* boundedness in time of Sobolev norms, and thereby allow the local well posedness

to be extended to arbitrary time. Suppose an initial datum u_0 is given in $H^{1/2}$, say. Then since the $H^{1/2}$-norm dominates the L^3-norm in one dimension by fractional Sobolev estimates (see [16]), we have $I_0(u_0) < \infty$ and $I_1(u_0) < \infty$. Consider the estimate

$$\begin{aligned}
\|u(\cdot,t)\|^2_{H^{1/2}} &= \int u^2(x,t)\,dx + \int u(x,t)Hu_x(x,t)\,dx \\
&= I_0(u_0) - I_1(u_0) + \tfrac{1}{3}\int u^3(x,t)\,dx \\
&\le I_0(u_0) - I_1(u_0) + c\,\|u(\cdot,t)\|^3_{H^{1/6}} \\
&\le I_0(u_0) - I_1(u_0) + c\,\|u(\cdot,t)\|^2_{H^0}\|u(\cdot,t)\|_{H^{1/2}} \\
&= I_0(u_0) - I_1(u_0) + c\,I_0(u_0)\,\|u(\cdot,t)\|_{H^{1/2}}
\end{aligned}$$

Since $\|u(\cdot,t)\|^2_{H^{1/2}}$ is dominated by a quantity involving only $\|u(\cdot,t)\|_{H^{1/2}}$, it is clear that the $H^{1/2}$-norm stays bounded as long as the solution u exists. A similar argument shows that the H^1-norm stays bounded if the initial datum lies in H^1. In fact, it was proved in [1, 6, 18] that if initial data u_0 are given in $H^{n/2}$, where n is a positive integer, then there exists a weak solution in $L^\infty(\mathbb{R}, H^{n/2})$. Combining this result with the local existence theory of strong solutions in [1, 15], it is clear that if initial data with sufficient regularity are given, the problem (5) with $p = 1$ has global-in-time strong solutions that lie in $C([0,T], H^s)$ for $s > \frac{3}{2}$ and for $T > 0$.

If $p \ge 4$, global existence is known for small data, but for $p = 2$ and $p = 3$, the problem of global existence seems to be open even for small data. For an overview of known results and precise statements concerning regularity, the reader should consult [10] and [11]. It is worth mention that the main results of Molinet, Tzvetkov and Saut [11] indicate that local well-posedness results in H^s for $s < \frac{3}{2}$ are likely to be subtle. Reviewing these results, the question arises whether the lack of global well-posedness for arbitrary data if $p \ge 2$ is a technical problem, or whether it is prohibited by the existence of solutions which become unbounded in finite time. In the following, the goal is to indicate that the latter is indeed the case. If $p \ge 2$, the equation only has three known conserved integrals, *viz.*

$$\begin{aligned}
I_{-1}(u) &= \int u, \\
I_0(u) &= \int u^2, \\
I_1(u) &= \tfrac{2}{(p+1)(p+2)}\int u^{p+2} - \int uHu_x.
\end{aligned}$$

Unfortunately, it is not possible to adapt the preceeding argument that was effective when $p = 1$ to the cases where $p \ge 2$, as the resulting inequality is not sufficient to control the $H^{1/2}$-norm. To gain some insight into this issue, we initiate a numerical study of the equation.

3. **Discretization of the periodic Benjamin-Ono equation.** The question outlined above will be considered in the periodic context. Consider the initial-value problem

$$\left.\begin{aligned}
&u_t + u^p u_x - Hu_{xx} = 0, \qquad x \in [0,2\pi],\ t \ge 0, \\
&u(x,0) = u_0(x), \\
&u(0,t) = u(2\pi,t).
\end{aligned}\right\} \tag{6}$$

As was mentioned, the approach is via numerical simulation, and it is our purpose now to describe the discretization of the periodic initial-value problem (6). Because the Hilbert transform H has a convenient formulation in terms of the Fourier transform, a Fourier-collocation method is a natural choice. Such methods have been developed for evolution equations generally (see [5]), and for the Benjamin-Ono equation with $p = 1$ in [13] and [17]. In consequence, an abbreviated description seems appropriate.

Denote by S_N the subspace of L^2 spanned by the set of functions

$$\{e^{ikx} \ : \ k \in \mathbb{Z}, \ -N \leq k \leq N\},$$

and define the collocation points to be $x_j = \frac{2\pi j}{N}$ for $j = 0, 1, ...N-1$. Let I_N be the interpolation operator from $H^1_{\#}([0, 2\pi])$ onto S_N. Writing the approximate semi-discrete solution $u_N \in C(0, T, S_N)$ as

$$u_N(x,t) = \sum_{k=-\frac{N}{2}}^{\frac{N}{2}-1} \tilde{u}_N(k,t) e^{ikx}, \tag{7}$$

the discretization is effected by enforcing the equation

$$\left.\begin{array}{c} (\partial_t u_N + \frac{1}{2}\partial_x(u_N^2) - \partial_x^2 H u_N)(x_j, t) = 0, \qquad t \in [0, T] \\ u_N\big|_{t=0} = I_N u_0 \in S_N, \end{array}\right\} \tag{8}$$

for $0 \leq j \leq N-1$. Using the definition (7) of u_N in (8) yields a system of ordinary differential equations for the discrete Fourier coefficients $\tilde{u}_N(k,t)$. To solve this system of equations, a first-order implicit Runge-Kutta method is used. The general n-stage implicit Runge-Kutta method is characterized by the tableau

$$\begin{array}{c|c} A & \tau \\ \hline b^T & \end{array},$$

where A is an n-by n matrix, and b and τ are n-vectors. A general outline of the theory and application of implicit Runge-Kutta methods can be found in [3, 4], and the references contained in these articles. The 1-stage method used in this report is characterized by the tableau

$$\begin{array}{c|c} \frac{1}{2} & \frac{1}{2} \\ \hline 1 & \end{array}.$$

A higher-order method could be used, but the additional stability offered by the second-order method argued in its favor. Moreover, in order to observe singularity formation, the time step has to be extremely small, regardless of the order of the time discretization. The fully discrete approximation to u at the the nth time step will be denoted by U_N^n. Given U_N^n and the size of the time step h, the solution at the next time-step is computed according to

$$U_N^{n+1} = U_N^n + \ h \ F(X, n+1/2),$$

$$X = U_N^n + \tfrac{1}{2} h \ F(X, n+1/2),$$

where

$$F(X, n) = F(X) = H\partial_x^2(X) - \tfrac{1}{2}\partial_x((X)^2).$$

Observe that F does not depend explicitly on time in this case. Moreover, the time-stepping is actually made in terms of the Fourier coefficients via the relations

$$\begin{aligned}\tilde{U}_N^{n+1}(k) &= \tilde{U}_N^n(k) + i\,h\left\{\,|k|k\tilde{X}(k) - \tfrac{1}{2}k(\tilde{X}\star\tilde{X})(k)\right\}\\ \tilde{X}(k) &= \tilde{U}_N^n(k) + i\,\frac{h}{2}\left\{\,|k|k\tilde{X}(k) - \tfrac{1}{2}k(\tilde{X}\star\tilde{X})(k)\right\}\end{aligned}$$

The convolution is evaluated pseudospectrally, and $\tilde{X}$ is approximated iteratively. In practice it has been found that four iterations are sufficient to obtain the formal 2^{nd}-order convergence rate. Moreover, as mentioned before, the time step has to be extremely small. Therefore at each new time step, one already has in hand a very good starting point for the iteration.

Although no attempt has been made to give a formal proof of the convergence of the solution U_N of the discrete problem to the solution u of the initial-value problem (6), the convergence of the scheme was tested in some detail.

4. **Convergence Study.** For equation (6) with $p = 1$, there are exact solutions in the form of periodic traveling waves. These solutions, found by Benjamin [2], are given by the formula

$$u(x,t) = \frac{\sinh(\lambda)}{\cosh^2(\frac{\lambda}{2}) - \cos^2(\frac{x-ct}{2})}, \tag{9}$$

with speed

$$c = \frac{1}{\tanh(\lambda)}. \tag{10}$$

Figure 1 shows a typical periodic traveling wave which can be used to test the numerical algorithm in the case $p = 1$. The norm used to calculate the error is the discrete L^2-norm

$$\|u\|_{N,2}^2 = \frac{1}{N}\sum_{i=1}^{N}|u(x_i)|^2.$$

The normalized L^2-error is then defined by

$$E_2 = \frac{\|u - U_N\|_{N,2}}{\|u\|_{N,2}}.$$

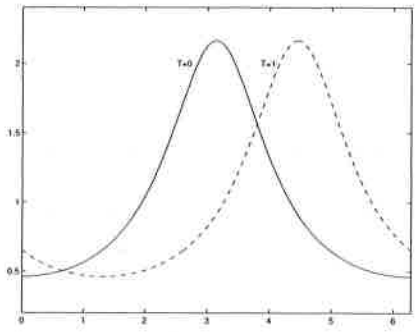

FIGURE 1. Traveling-wave solution to (6) with $p = 1$, $\lambda = 1$ and $c = 1.313$.

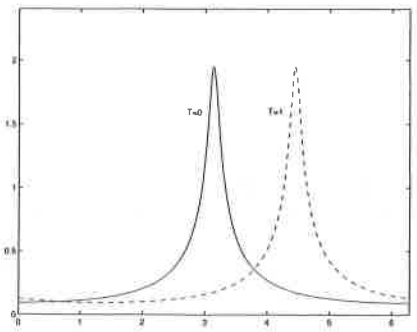

FIGURE 2. Approximate traveling-wave solution to (6) with $p = 3$ and $c = 1.313$.

h	L^2-Error	Ratio
0.1000	4.194e-03	
0.0500	8.299e-04	5.05
0.0250	1.915e-04	4.33
0.0125	4.733e-05	4.05
0.0063	1.182e-05	4.00
0.0031	2.956e-06	4.00

N	L^2-Error	Ratio
8	2.96e-01	
16	2.52e-02	11.76
32	1.25e-05	201.43
64	3.41e-09	366.62
128	3.41e-09	1.00

TABLE 1. Discretization error for a traveling wave as in (9) with $\lambda = 0.7$ over the time domain $[0, 1]$. In the left table, the number of grid points is $N = 1024$. In the right table, the time step is $h = 4 * 10^{-5}$.

h	L^2-Error	Ratio
0.1000	2.196e-03	
0.0500	4.886e-04	4.49
0.0250	1.205e-04	4.05
0.0125	3.013e-05	4.00
0.0063	7.534e-06	4.00
0.0031	1.883e-06	4.00

h	L^2-Error	Ratio
0.1000	7.521e-02	
0.0500	3.213e-02	2.34
0.0250	5.826e-03	5.51
0.0125	1.033e-03	5.64
0.0063	3.582e-04	2.88
0.0031	2.316e-04	1.55

TABLE 2. The generalized Benjamin-Ono equation with $p = 3$: Error when the solution is $u(x, t) = \cos(x - t)$ (left) or an approximate traveling wave (right). The time domain is $[0, 1]$, and the number of grid points is $N = 1024$ in the left table, and $N = 4096$ in the right table.

To obtain the results shown in Table 1, a traveling wave with $\lambda = 0.7$ was used. As can be seen, for this function, the error decreases quadratically with the size of the time step, and the error decreases spectrally with the number of modes used. A similar convergence result obtains using a smaller time step and a higher number of modes.

In the case when $p \neq 1$, no exact formula for a traveling wave is known. However, the algorithm can be tested using the inhomogeneous problem

$$\left.\begin{array}{c} u_t + u^p u_x - H u_{xx} = f(x,t), \\ u(x,0) = \phi(x). \end{array}\right\} \tag{11}$$

Table 2 contains some results for $p = 3$ when the solution of (11) is a cosine function. Here, the time domain was $[0, 1]$, and the number of grid points was $N = 1024$. In this case as well, the error decreases quadratically in the size of the time step. The second part of Table 2 shows the error when initial data are taken to be a numerical approximation of a traveling wave for (6) with $p = 3$ (see Figure 2). It is again apparent that the temporal scheme is second-order convergent in the size of the time step h. However in this case, the accuracy is limited by the accuracy of the approximate traveling wave used as initial data. The approximation to the traveling wave was found by a modified Newton's method which will be reported elsewhere.

As another measure of how well the discrete solution approximates the actual solution, we monitored the first three conserved integrals at time $T = 1$. Table 3 shows the conservation of these integrals for a traveling wave with $\lambda = 1$ from $T = 0$

h	N	I_{-1}	I_0	I_1
0.002	2048	1e-15	9.834e-12	1.642e-11
0.002	4096	1e-15	9.828e-12	1.640e-11
0.0002	4096	2e-15	1.013e-15	3.115e-15
0.0002	8192	1e-15	3.660e-15	4.032e-15

TABLE 3. Benjamin-Ono equation: Conservation of integrals for a traveling-wave solution. In each box, the difference between the computed value at $T = 0$, and the value at $T = 1$ is shown.

h	N	I_{-1}	I_0	I_1
0.002	2048	1e-15	7.587e-14	2.0598e-08
0.002	4096	1e-15	7.587e-14	2.0598e-08
0.0002	4096	3.887e-15	7.570e-15	2.059e-10
0.0002	8192	3.887e-15	7.570e-15	2.059e-10
0.00002	8192	3.887e-15	1e-15	2.065e-12

TABLE 4. Benjamin-Ono equation: Conservation of integrals for a general solution. In each box, the difference between the computed value at $T = 0$, and the value at $T = 1$ is shown.

h	N	I_{-1}	I_0	I_1
0.002	2048	1e-15	3.788e-13	4.684e-08
0.002	4096	1e-15	3.864e-13	4.684e-08
0.0002	4096	1e-15	1e-15	4.683e-10
0.0002	8192	1e-15	7.570e-15	4.684e-10

TABLE 5. Generalized Benjamin-Ono equation with $p = 3$: Conservation of integrals for a general solution. In each box, the difference between the computed value at $T = 0$, and the value at $T = 1$ is shown.

to $T = 1$ for different values of N and h. Table 4 shows the same quantities for the evolution of Gaussian initial data.

Since the traveling wave does not change its shape, better conservation is expected in the first case. A comparison of Tables 3 and 4 confirms this expectation. Thirdly, we investigate the numerical conservation of the integrals for the equation with $p = 3$. The conservation is slightly worse than for the case $p = 1$. The results in Table 5 are for a calculation in which the function stayed bounded. It can be shown that the integral, I_{-1} is conserved by the scheme up to round-off error, the error introduced by the iteration, and the error made in forming the integral. Thus it comes as no surprise that in all three cases the integral is conserved to within machine precision. On the other hand, the conservation of I_1 depends critically on the time step, in concert with the fact that this integral is not exactly conserved by the scheme. This observation will be useful later to provide a measure of accuracy for an adaptive algorithm.

5. **Simulation of blow-up.** Since it could not be determined theoretically whether a solution to (6) stays bounded if $p \geq 2$, it is natural to search for a solution that becomes unbounded in finite time. All results discussed here are for the case $p = 3$. The numerical simulation was started with a Gaussian profile

$$\phi(x) = Ae^{-\frac{(x-\pi)^2}{\lambda}} \tag{12}$$

as initial data. For small A and λ, the solution does not blow up, but rather evolves into a train of oscillations, propagating with a speed proportional to their frequency. This seems to confirm the heuristic that for small u, the equation is essentially linear, and the dominating effect is dispersion. To initiate blow-up, the mass $\int \phi(x)\,dx$ of the initial data was gradually increased by taking either A or λ larger. For initial data with sufficient mass, the solution steepens rapidly and forms a spike. This spike seems to be the initial stage of a solution which develops an L^∞-singularity in finite time. The blow-up is depicted in Figure 3. Figure 4 shows a close-up of Figure 3 (f). As can be seen, instability in the calculation is rapidly becoming a problem as the spike continues to grow, and the spatial and temporal gradients become large.

In an attempt to control the instability, an adaptive scheme was developed. To control the aliasing error, the tails of the discrete Fourier expansion of the approximate solution U_N^n are monitored. If the magnitude of the coefficients $\tilde{U}_N^{n+1}(k)$ in the tail of the expansion exceeds a specified tolerance TOL1, the calculation is stopped. The number of grid points is doubled, and U_N^n is interpolated to a function U_{2N}^n, given on the new grid. Then U_{2N}^{n+1} is computed. To limit the error due to the temporal discretization, the quality of the conservation of the integral

$$I_1(U_N^{n+1}) = \int \tfrac{1}{10}(U_N^{n+1})^5 - U_N^{n+1} H\partial_x U_N^{n+1}\,dx$$

is tested at each time step. Since this integral is a difference of two quantities that both become unbounded, the conservation of the integral is a good indication of the stability of the calculation. If the difference

$$\left|I_1(U_N^{n+1}) - I_1(U_N^n)\right|$$

is larger than the tolerance TOL2, the time step h is halved and U_N^{n+1} is recalculated. The adaptive algorithm is depicted in the diagram in Figure 6. The tolerances TOL1 and TOL2 were chosen after extensive experimentation. A rough guide to what the values should be can be gleaned from [3], where a related scheme for the generalized Korteweg-de Vries equation was implemented. In our calculations, TOL1 was taken in the range 0.01 to 0.03, and TOL2 was taken between 10^{-7} and $3 * 10^{-7}$.

To get an idea of how well the adaptive algorithm performs, results of a run are presented in the next table. It can be seen that the integral I_1 is conserved to 4 decimal places, while the maximum of the solution approaches 50. Using this adaptive algorithm, further simulations were carried out. It appeared that the adaptive procedure was sufficient to control instability in the numerically generated approximation. However, due to computer storage limitations, the maximum size of a solution was limited to approximately 50. Nevertheless, even at this modest level, it is apparent in Figure 7 that the solution develops a similarity structure in a neighborhood of the blow-up point. To further quantify the blow-up, several experiments were conducted with the aim of establishing the rates at which various norms tend to infinity as the blow-up time is approached. For instance, suppose

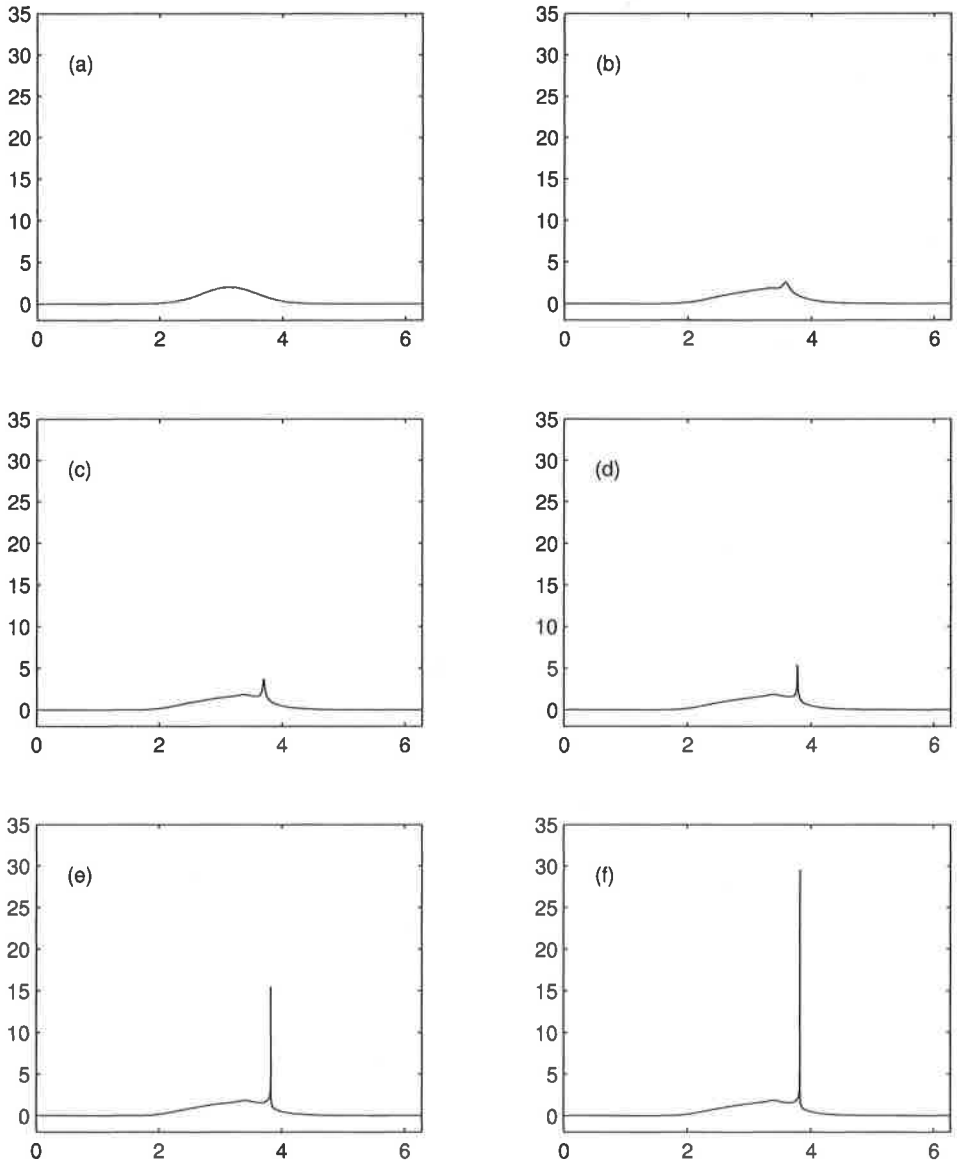

FIGURE 3. Blow-up of Gaussian initial data with $A = 2$ and $\lambda = 0.5$. This is a calculation with fixed values $N = 2^{19}$ and $h = 4 \times 10^{-8}$. The times shown are (*a*) $t = 0$, (*b*) $t = 0.018349609375$, (*c*) $t = 0.024794921875$, (*d*) $t = 0.0268203125$, (*e*) $t = 0.02721823120117$, (*f*) $t = 0.02721904736328$.
Although not visible here, this calculation is suffering from instability due to aliasing errors (see close-up in Figure 4).

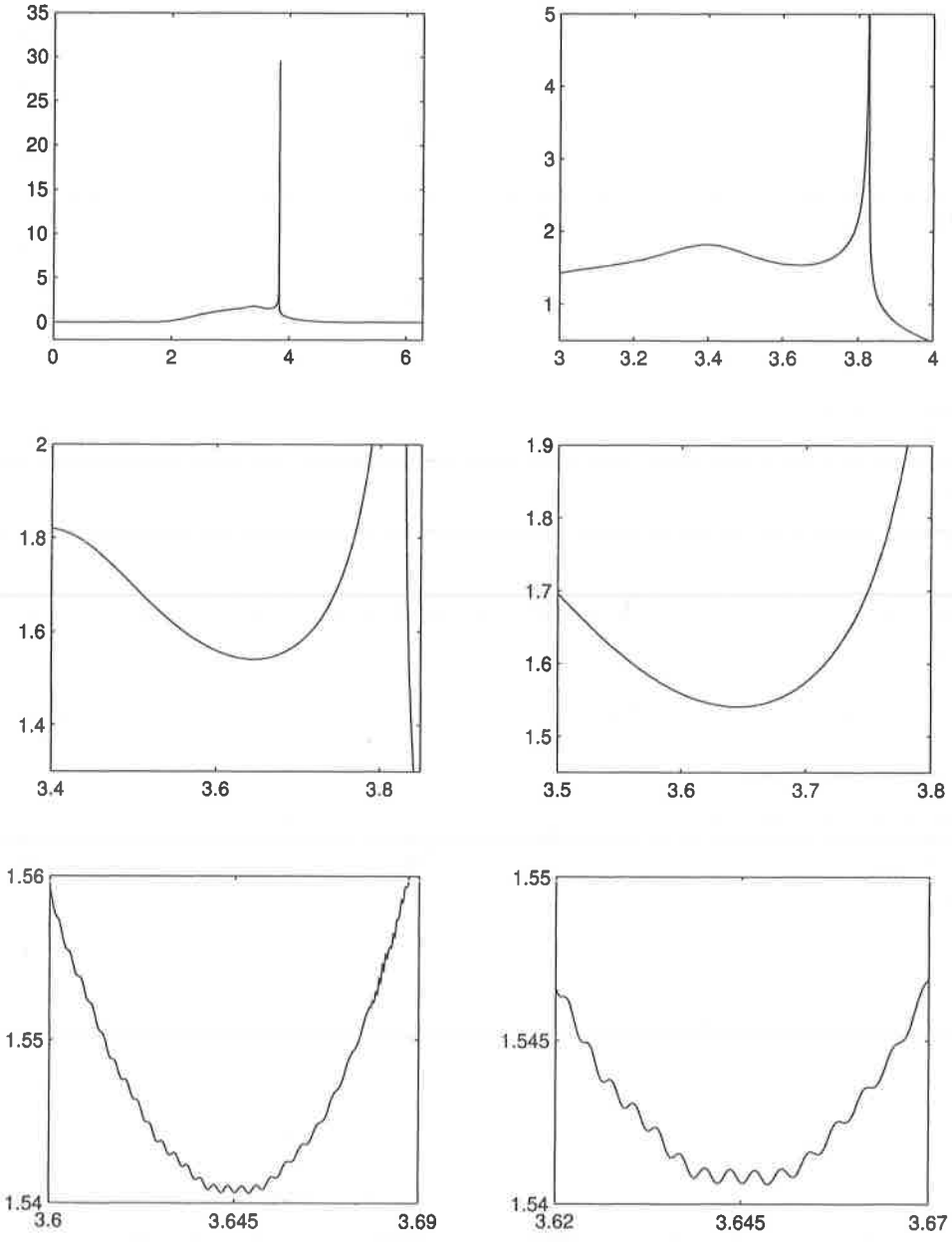

FIGURE 4. Blow-up of Gaussian initial data with $A = 2$ and $\lambda = 0.5$: Instability. This is the same calculation as in Figure 3, but a close-up is shown at at time $t = 0.02723337891102$. The spurious oscillations are a clear sign of computational instability due to aliasing errors.

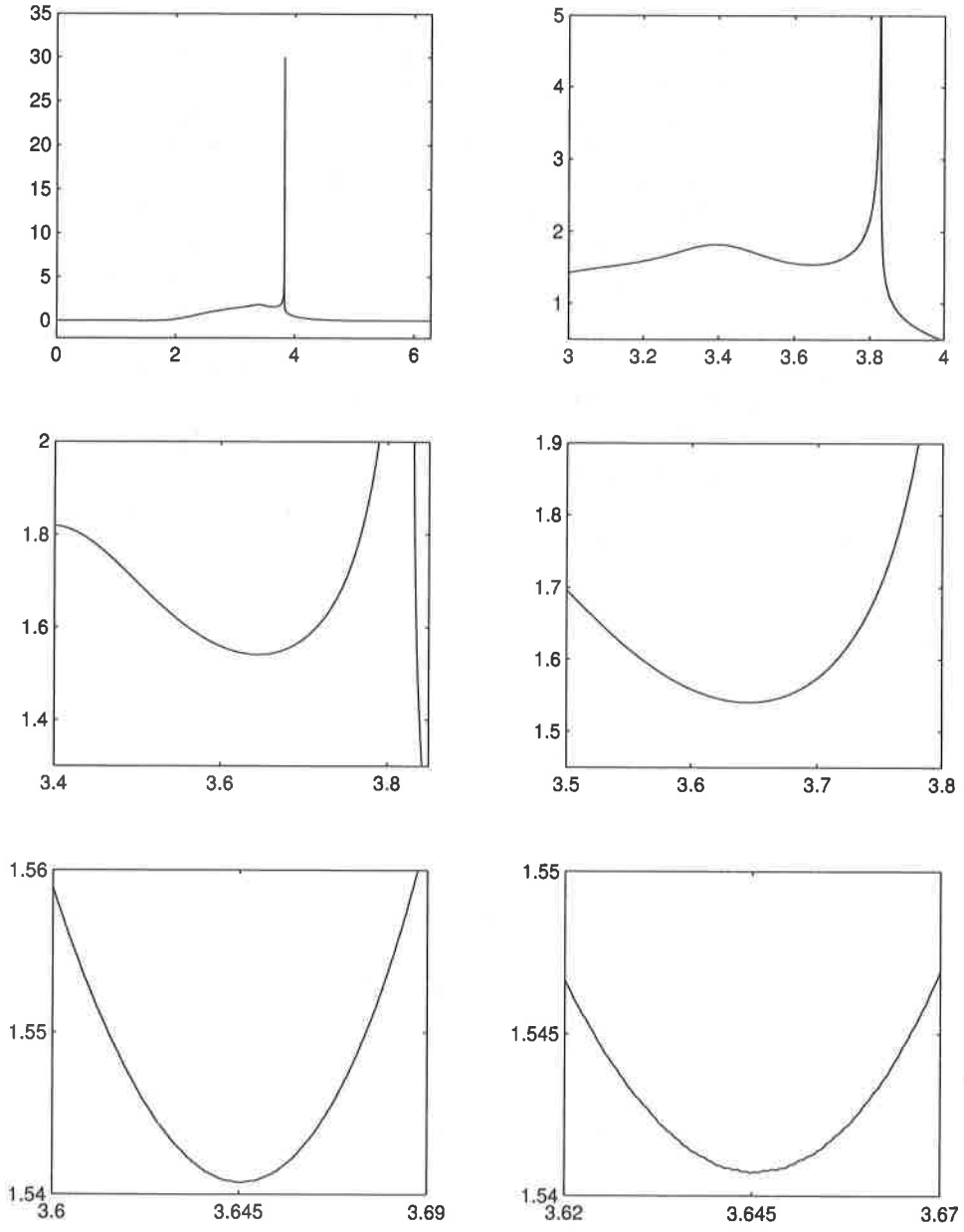

FIGURE 5. Blow-up of Gaussian initial data with $A = 2$ and $\lambda = 0.5$. This is the same calculation as shown in Figures 3 and 4, but using the adaptive algorithm. A close-up is shown at at time $t = 0.02723337891102$. Note that the adaptive algorithm has effectively removed the instability which was evident in the previous figure.

t	$I_{-1}(u_N)$	$I_1(u_N)$	$L^\infty(u_N(\cdot,t))$
0.0178500000000	2.24199648655437	12.76556	2.690144
0.0227125000000	2.24199648655436	12.76562	3.589563
0.0244656250000	2.24199648655437	12.76571	4.623624
0.0251953437500	2.24199648655436	12.76583	6.993904
0.0252592500000	2.24199648655437	12.76599	8.680310
0.0252799562500	2.24199648655438	12.76614	11.499567
0.0252835600000	2.24199648655441	12.76638	14.393761
0.0252844760000	2.24199648655441	12.76657	17.685924
0.0252847657875	2.24199648655436	12.76473	23.039991
0.0252848298250	2.24199648655438	12.76525	31.482316
0.0252848363350	2.24199648655441	12.75494	40.078124
0.0252848399500	2.24199648655436	12.75538	49.339268
0.0252848406250	2.24199648655437	12.75562	50.023054

TABLE 6. Evolution of Gaussian initial data with $A = 2$ and $\lambda = 0.4$ using the adaptive algorithm: Conservation of integrals and blow-up of the L^∞-norm.

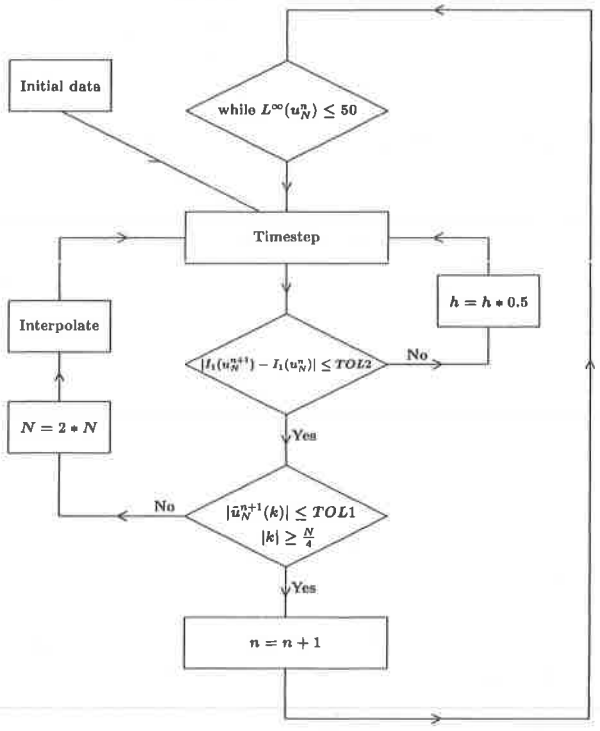

FIGURE 6. Adaptive algorithm.

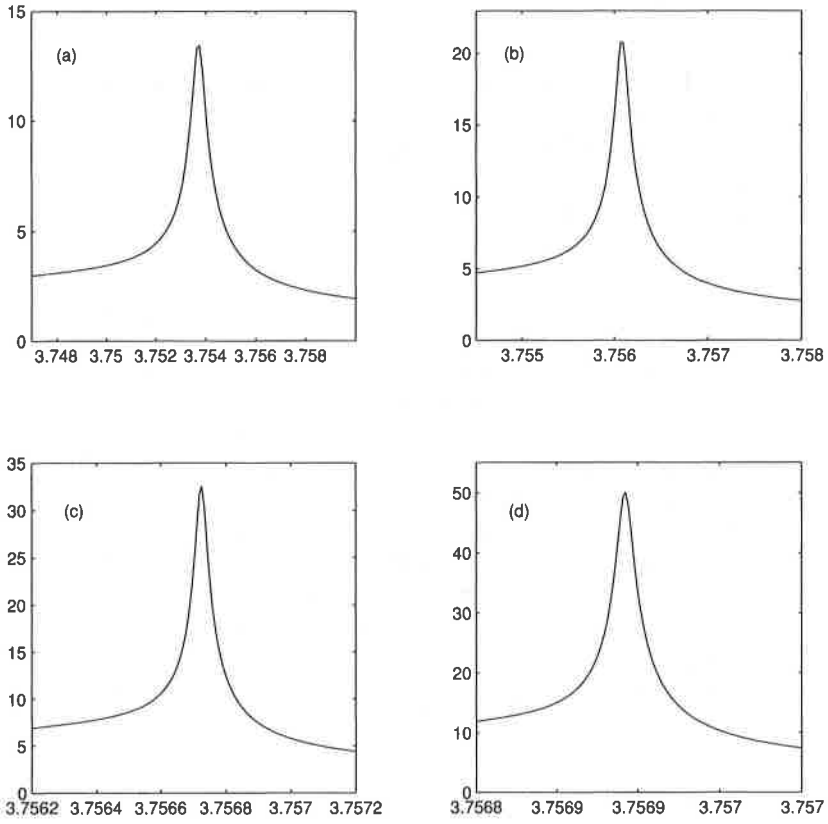

FIGURE 7. Blow-up of Gaussian initial data with $A = 2$ and $\lambda = 0.4$: Similarity Structure, (a) $t = 0.02528299$, (b) $t = 0.0252846919375$, (c) $t = 0.025284831975$, (d) $t = 0.025284840687971$.

that the L^∞-norm behaves like

$$M(t) = \|u_N(\cdot, t)\|_\infty = c(t^* - t)^{-\rho}.$$

If the quantity $M(t)$ is known at two different times t_i and t_{i+1}, and if the blow-up time t^* is known, then the exponent ρ can be computed approximately to be

$$\rho_i = -\frac{\log(M(t_i/M(t_{i+1}))}{\log((t^* - t_i)/(t^* - t_{i+1})}. \tag{13}$$

Of course, the time t^* is not known and must be estimated. In our experiments, we took it that the solution was infinite when it reached a height of 50. The rates ρ_i are calculated only for times safely away from the blow-up time t^*.

A second set of experiments was performed using the approximate traveling-wave solutions mentioned earlier in the context of the convergence study. These waves were perturbed slightly with a Gaussian profile in order to facilitate the development of a singularity. The resulting blow-up is shown in Figure 10.

6. **Blow-up rates.** After some preliminary numerical computations, it appeared that the blow-up takes place in the form of a similarity structure as indicated in

i	L^4	L^5	L^6	L^∞	$L^{2,D}$
6	3.71e-03	5.06e-02	8.43e-02	2.05e-01	5.42e-01
7	-2.09e-0	4.95e-02	8.31e-02	1.79e-01	5.09e-01
8	-6.00e-0	4.99e-02	8.24e-02	1.96e-01	4.81e-01
9	1.06e-02	5.81e-02	8.45e-02	1.77e-01	4.63e-01
10	2.11e-02	6.19e-02	8.51e-02	1.78e-01	4.55e-01
11	2.89e-02	6.42e-02	8.50e-02	1.68e-01	4.46e-01
12	3.34e-02	6.52e-02	8.45e-02	1.88e-01	4.38e-01
13	3.51e-02	6.55e-02	8.42e-02	1.73e-01	4.34e-01
14	3.67e-02	6.57e-02	8.38e-02	1.67e-01	4.30e-01
15	3.79e-02	6.58e-02	8.35e-02	1.70e-01	4.26e-01
16	3.84e-02	6.58e-02	8.33e-02	1.73e-01	4.24e-01
17	3.90e-02	6.59e-02	8.32e-02	1.63e-01	4.22e-01
18	3.95e-02	6.59e-02	8.30e-02	1.65e-01	4.20e-01
19	3.98e-02	6.59e-02	8.30e-02	1.85e-01	4.19e-01
20	4.00e-02	6.60e-02	8.29e-02	1.65e-01	4.18e-01
21	4.04e-02	6.60e-02	8.29e-02	1.63e-01	4.17e-01
22	4.06e-02	6.61e-02	8.28e-02	1.69e-01	4.16e-01
23	4.08e-02	6.61e-02	8.28e-02	1.67e-01	4.13e-01
24	4.09e-02	6.60e-02	8.26e-02	1.65e-01	3.98e-01
25	4.08e-02	6.57e-02	8.22e-02	1.64e-01	3.58e-01
	$0.041\bar{6}$	$0.0\bar{6}$	$0.08\bar{3}$	$0.1\bar{6}$	$0.41\bar{6}$

TABLE 7. Blow up of Gaussian initial data with $A = 2$ and $\lambda = 0.4$. The number in each slot represents the blow-up rate ρ_i for the respective quantity, calculated at the i-th time the time step was halved. $L^{2,D}$ denotes the L^2-norm of the discrete derivative of u_N. The starting values for the time step and the number of grid points were $h = 5 * 10^{-5}$ and $N = 4096$, respectively. The tolerances were TOL1 $= 10^{-2}$ and TOL2 $= 10^{-7}$. The numbers at the bottom are the exponents predicted by the similarity structure (14).

Figure 7. Assuming the blow-up occurs at time $t^*$and the solution develops a single infinite peak at $x = x^*$, the solution appears to have the form

$$u(x,t) \cong \frac{1}{(t^*-t)^{\frac{1}{2p}}}\phi\Big(\frac{x^*-x-c(t^*-t)^{1/2}}{(t^*-t)^{1/2}}\Big), \tag{14}$$

in the immediate vicinity of the maximum of the function. Defining the variable

$$\xi = \frac{x^*-x}{(t^*-t)^{\frac{1}{2}}} - c,$$

it is straightforward to determine that ϕ satisfies the equation

$$\frac{1}{2p}\phi + \frac{1}{2}(\xi+c)\phi' - \phi^p\phi' + H\phi'' = 0.$$

The detailed analysis of this equation will be the focus of future work. In the present context, the similarity structure is useful for predicting the blow-up rates appearing

i	L^4	L^5	L^6	L^∞	$L^{2,D}$
6	9.94e-04	4.99e-02	8.37e-02	2.01e-01	5.28e-01
7	-5.22e-03	4.87e-02	8.25e-02	1.77e-01	4.99e-01
8	-1.58e-03	5.24e-02	8.30e-02	1.92e-01	4.74e-01
9	1.78e-02	6.08e-02	8.50e-02	1.71e-01	4.58e-01
10	2.95e-02	6.43e-02	8.49e-02	1.79e-01	4.45e-01
11	3.46e-02	6.54e-02	8.43e-02	1.71e-01	4.36e-01
12	3.68e-02	6.57e-02	8.38e-02	1.69e-01	4.29e-01
13	3.82e-02	6.58e-02	8.34e-02	1.70e-01	4.24e-01
14	3.90e-02	6.59e-02	8.32e-02	1.65e-01	4.21e-01
15	3.96e-02	6.59e-02	8.30e-02	1.70e-01	4.19e-01
16	4.00e-02	6.60e-02	8.29e-02	1.67e-01	4.18e-01
17	4.03e-02	6.60e-02	8.29e-02	1.67e-01	4.17e-01
18	4.03e-02	6.60e-02	8.28e-02	1.63e-01	4.15e-01
19	4.01e-02	6.59e-02	8.27e-02	1.57e-01	4.10e-01
20	3.89e-02	6.56e-02	8.25e-02	1.72e-01	3.88e-01
21	2.76e-02	6.32e-02	8.16e-02	1.61e-01	3.39e-01
22	5.66e-02	6.78e-02	8.17e-02	1.70e-01	2.69e-01
23	4.36e-02	6.42e-02	7.97e-02	1.57e-01	1.90e-01
24	4.19e-02	6.29e-02	7.83e-02	1.40e-01	1.48e-01
25	4.06e-02	6.14e-02	7.64e-02	1.58e-01	1.12e-01
	$0.041\bar{6}$	$0.0\bar{6}$	$0.08\bar{3}$	$0.1\bar{6}$	$0.41\bar{6}$

TABLE 8. Blow up of Gaussian initial data with $A = 2$ and $\lambda = 0.4$. The number in each slot represents the blow-up rate ρ_i for the respective quantity, calculated at the i-th time the time step was halved. $L^{2,D}$ denotes the L^2-norm of the discrete derivative of u_N. The starting values for the time step and the number of grid points were $h = 5 * 10^{-5}$ and $N = 4096$, respectively. The tolerances were TOL1 $= 2 * 10^{-2}$ and TOL2 $= 2 * 10^{-7}$. The numbers at the bottom are the exponents predicted by the similarity structure (14).

in (13). The form of the similarity solution suggests the following power laws for the L^q-norms of the solution:

$$\|u(\cdot,t)\|_{L^q} = c_q(t^* - t)^{\frac{1}{2q}-\frac{1}{2p}},$$

$$\|u(\cdot,t)\|_{L^\infty} = c_\infty(t^* - t)^{-\frac{1}{2p}}.$$

Moreover, the L^2-norm of the derivative is also of interest. The similarity structure predicts the relation

$$\|u_x(\cdot,t)\|_{L^2} = C_2(t^* - t)^{-\frac{1}{2p}-\frac{1}{4}}.$$

Using these power laws, the blow-up rate for the L^p-norms and the L^2-norm of the derivative can be predicted. The results of several calculations, shown in Tables 7 ,8 and 9, are compared to the predictions. All simulations are for equation (6) with $p = 3$. The first two tables show calculations with Gaussian initial data using different tolerances. As can be seen, the blow-up rates agree to one or two

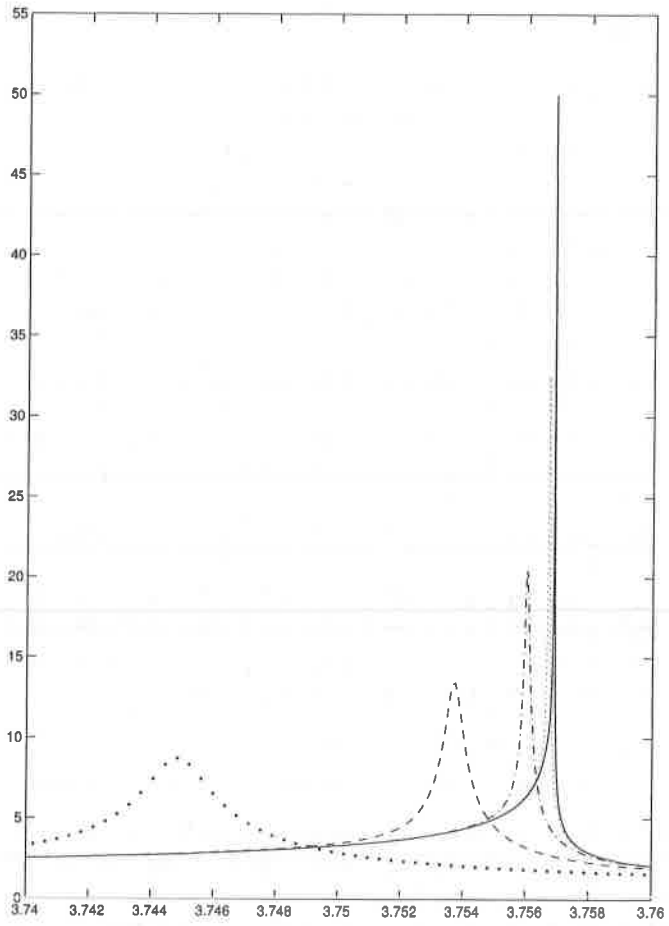

FIGURE 8. Blow-up of Gaussian initial data with $A = 2$ and $\lambda = 0.4$ using the adaptive algorithm. $(\bullet\bullet)$ $t = 0.02525965625$, $(--)$ $t = 0.02528299$, $(-\cdot)$ $t = 0.0252846919375$, $(\cdot\cdot)$ $t = 0.025284831975$, $(-)$ $t = 0.025284840687971$.

decimal places. The third table shows a computation with a perturbed approximate traveling wave. In this case, the blow-up rates are in even better agreement with the numbers predicted by the similarity structure.

In conclusion, the experiments shown in this report present evidence that solutions to (6) may become unbounded in finite time. Thus it is conjectured that (6) is not globally well-posed when $p = 3$, or indeed when $p \geq 2$.

REFERENCES

[1] L. Abdelouhab, J. L. Bona, M. Felland and J.-C. Saut, NONLOCAL MODELS FOR NONLINEAR DISPERSIVE WAVES, Physica D, 40 (1989), 360–392.

[2] T.B. Benjamin, INTERNAL WAVES OF PERMANENT FORM IN FLUIDS OF GREAT DEPTH, J. Fluid Mechanics, (1967) 29, 559–592

[3] J.L. Bona, V.A. Dougalis, O.A. Karakashian and W.R. McKinney, CONSERVATIVE, HIGH-ORDER NUMERICAL SCHEMES FOR THE GENERALIZED KORTEWEG-DE VRIES EQUATION, Philos. Trans. Royal Soc. London Ser. A, 351 (1995), 107–164.

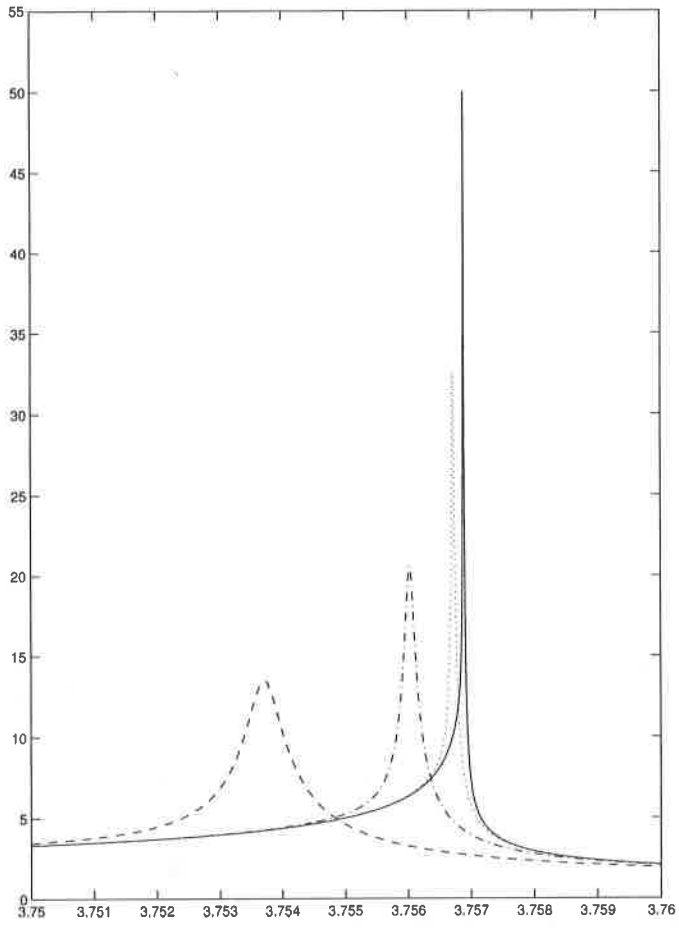

FIGURE 9. Blow-up of Gaussian initial data with $A = 2$ and $\lambda = 0.4$, close-up. $(--)$ $t = 0.02528299$, $(-\cdot)$ $t = 0.0252846919375$, $(\cdot\cdot)$ $t = 0.025284831975$, $(-)$ $t = 0.025284840687971$.

[4] J.C. Butcher, A CLASS OF IMPLICIT METHODS FOR ORDINARY DIFFERENTIAL EQUATIONS, Numerical analysis (Proc. 6th Biennial Dundee Conf., Univ. Dundee, Dundee, 1975), 28-37. Lecture Notes in Math. 506, Springer: Berlin, 1976.

[5] C. Canuto, M. Y. Hussaini, A. Quarteroni and T.A. Zang, SPECTRAL METHODS IN FLUID DYNAMICS, Springer: Berlin, 1988.

[6] J. Ginibre and G. Velo, SMOOTHING PROPERTIES AND EXISTENCE OF SOLUTIONS FOR THE GENERALIZED BENJAMIN-ONO EQUATION, J. Diff. Eq., 93 (1991), 150–212.

[7] R.J. Iorio, THE BENJAMIN-ONO EQUATION IN WEIGHTED SOBOLEV SPACES, J. Math. Anal. Appl., 157 (1991), 577–590.

[8] R.J. Iorio, ON THE CAUCHY PROBLEM FOR THE BENJAMIN-ONO EQUATION, Comm. Partial Diff. Eq., 11 (1986), 1031–1081.

[9] H. Kalisch and J.L. Bona, MODELS FOR INTERNAL WAVES IN DEEP WATER, Disc. Cont. Dyn. Syst., 6 (2000), 1–20.

[10] C.E. Kenig, G. Ponce, and L. Vega, ON THE GENERALIZED BENJAMIN-ONO EQUATION, Trans. American Math. Soc., 342 (1994), 155–172.

[11] L. Molinet, J.C. Saut and N. Tzvetkov, ILL-POSEDNESS ISSUES FOR THE BENJAMIN-ONO AND RELATED EQUATIONS, SIAM J. Math. Anal., 33 (2001), 982–988.

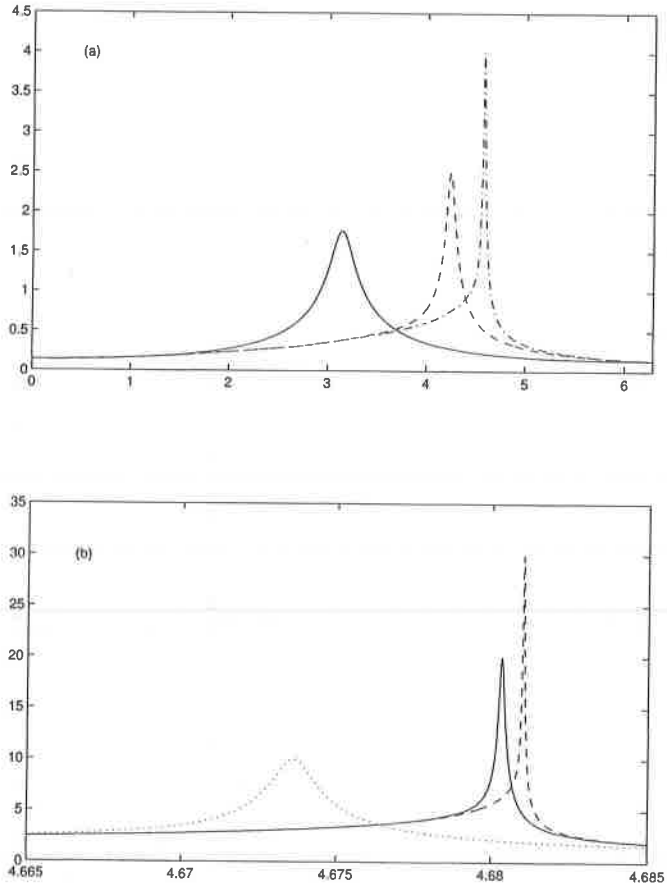

FIGURE 10. Blow-up for initial data taken to be a perturbation of the traveling wave shown in Figure 2. (a) : $(-)$ $t = 0$, $(--)$ $t = 0.61357421875$; $(-\cdot)$ $t = 0.6569335938$. (b) : $(\cdot\cdot)$ $t = 0.6589028702$, $(-)$ $t = 0.6589135569$, $(--)$ $t = 0.6589137413$.

[12] H. Ono, ALGEBRAIC SOLITARY WAVES IN STRATIFIED FLUIDS, J. Phys. Soc. of Japan, 39 (1975), 1082–1091.

[13] B. Pelloni, and V.A. Dougalis, ERROR ESTIMATES FOR A FULLY DISCRETE SPECTRAL SCHEME FOR A CLASS OF NONLINEAR, NONLOCAL DISPERSIVE WAVE EQUATIONS, Appl. Numer. Math., 37 (2001), 95–107.

[14] G. Ponce, SMOOTHING PROPERTIES OF SOLUTIONS TO THE BENJAMIN-ONO EQUATION, In Analysis and Partial Differential Equations (ed. C. Sadovsky) Lecture Notes in Pure & Appl. Math. 122, Dekker: New York (1990), 667–679.

[15] G. Ponce, ON THE GLOBAL WELL-POSEDNESS OF THE BENJAMIN-ONO EQUATION, Differential & Integral Eq., 4 (1991), 527–542.

[16] E.M. Stein, SINGULAR INTERGRALS AND DIFFERENTIABILITY PROPERTIES OF FUNCTIONS, Princeton Mathematical Series 30, Princeton University Press, Princeton, N.J. 1970.

[17] V. Thomeé and A.S. Vasudeva Murthy, A NUMERICAL METHOD FOR THE BENJAMIN-ONO EQUATION, BIT, 38 (1998), 597–611.

[18] M.M. Tom, SMOOTHING PROPERTIES OF SOME WEAK SOLUTIONS OF THE BENJAMIN-ONO EQUATION, Diff. Integral Eq., 3 (1990), 683–694.

Received March 2002; revised October 2003; final version February 2004.

i	L^4	L^5	L^6	L^∞	$L^{2,D}$
6	4.71e-02	6.88e-02	8.45e-02	1.66e-01	4.08e-01
7	4.68e-02	6.89e-02	8.48e-02	1.68e-01	4.13e-01
8	4.63e-02	6.87e-02	8.49e-02	1.67e-01	4.16e-01
9	4.59e-02	6.86e-02	8.48e-02	1.69e-01	4.18e-01
10	4.56e-02	6.84e-02	8.48e-02	1.69e-01	4.19e-01
11	4.53e-02	6.83e-02	8.47e-02	1.62e-01	4.19e-01
12	4.50e-02	6.81e-02	8.46e-02	1.68e-01	4.20e-01
13	4.48e-02	6.80e-02	8.44e-02	1.70e-01	4.20e-01
14	4.46e-02	6.78e-02	8.43e-02	1.71e-01	4.20e-01
15	4.43e-02	6.77e-02	8.42e-02	1.70e-01	4.19e-01
16	4.41e-02	6.76e-02	8.41e-02	1.58e-01	4.19e-01
17	4.39e-02	6.75e-02	8.40e-02	1.73e-01	4.19e-01
18	4.37e-02	6.74e-02	8.40e-02	1.61e-01	4.19e-01
19	4.35e-02	6.73e-02	8.39e-02	1.82e-01	4.19e-01
20	4.34e-02	6.72e-02	8.38e-02	1.66e-01	4.18e-01
21	4.33e-02	6.71e-02	8.37e-02	1.68e-01	4.18e-01
22	4.31e-02	6.70e-02	8.37e-02	1.63e-01	4.18e-01
23	4.30e-02	6.70e-02	8.36e-02	1.65e-01	4.18e-01
24	4.29e-02	6.69e-02	8.36e-02	1.71e-01	4.18e-01
25	4.28e-02	6.69e-02	8.35e-02	1.54e-01	4.17e-01
	$0.041\bar{6}$	$0.0\bar{6}$	$0.08\bar{3}$	$0.1\bar{6}$	$0.41\bar{6}$

TABLE 9. Blow-up rates for the perturbed traveling wave, as shown in Figure 10. The number in each slot represents the blow-up rate ρ_i for the respective quantity, calculated at the i-th time the time step was halved. $L^{2,D}$ denotes the L^2-norm of the discrete derivative of u_N. The starting values for the time step and the number of grid points were $h = 5 * 10^{-5}$ and $N = 4096$, respectively. The tolerances were TOL1 $= 10^{-2}$ and TOL2 $= 2 * 10^{-7}$. The numbers at the bottom are the exponents predicted by the similarity structure (14).

E-mail address: bona@math.uic.edu
E-mail address: kalisch@maths.lth.se
Received March 2003; revised October 2003; final version February 2004.